Evaluation of Geometrically Nonlinear Reduced Order Models with Nonlinear Normal Modes

Robert J. Kuether[*]
Engineering Physics Department, University of Wisconsin-Madison, Madison, Wisconsin, 53706
Brandon J. Deaner[†]
Mercury Marine, Fond du Lac, Wisconsin, 54936
Joseph J. Hollkamp[‡]
U.S. Air Force Research Laboratory, Wright-Patterson Air Force Base, Ohio, 45433
and
Matthew S. Allen[§]
Engineering Physics Department, University of Wisconsin-Madison, Madison, Wisconsin, 53706

In the past few decades several reduced order modeling (ROM) strategies have been developed which can create low order models of geometrically nonlinear structures from detailed finite element models. These methods can provide very accurate results at a dramatically reduced computational cost, but it is often not straightforward to determine which modes must be included in the reduced order model to obtain accurate results. Furthermore, the reduced models are estimated by applying a series of static loads to the finite element model, and the results can be sensitive to the amplitudes of the static loads that are used. Typically, this is addressed by integrating the full model subject to a small number of representative loading scenarios and its response is then compared with that computed by the candidate ROMs to evaluate their accuracy. This work proposes an alternative where the nonlinear normal modes (NNMs) of the structure are computed from each candidate ROM and compared to assess convergence. The NNMs are load independent properties of the system, and while superposition does not hold, if the NNMs coincide with the true NNMs over a range of frequency and energy then the model is at least guaranteed to correctly capture the response in a large number of important conditions.

[*] Graduate Research Assistant, 534 Engineering Research Building, 1500 Engineering Drive, Madison, WI 53706-1609, rkuether@wisc.edu.
[†] Structural Analyst, W6250 Pioneer Road, Fon du Lac, WI 54936, Brandon.Deaner@mercmarine.com.
[‡] Senior Aerospace Engineer, Structural Sciences Center, AFRL/RQHF, 2790 D Street, Building 65, Wright-Patterson Air Force Base, OH 45433, Joseph.Hollkamp@us.af.mil.
[§] Associate Professor, 535 Engineering Research Building, 1500 Engineering Drive, Madison, WI 53706-1609, msallen@engr.wisc.edu, AIAA Lifetime Member.

Keywords: reduced order models, nonlinear normal modes, geometric nonlinearities, periodic orbits, finite element analysis.

I. Introduction

In structural dynamics, linear normal modes of vibration provide important insights into the behavior of a structure modeled under the assumption of linearity. In the presence of nonlinearity, the nonlinear normal mode (NNM) offers a different theoretical definition of a vibration mode that can be used to understand the behavior of a system, while maintaining a conceptual similarity to linear vibration modes. Consider the thin-walled skin panels of a high speed aircraft that experiences extreme pressure and thermal loads due to the flow field and engine noise [1]. These panels may vibrate nonlinearly with large amplitudes in response to the large pressure fluctuations, and can even vibrate about a buckled equilibrium position. Using the assumption of linearity to analyze the response and life of these geometrically nonlinear panels would result in an overly conservative design, at best [2]. When modeling complicated structures such as these skin panels, the finite element method is used extensively in industry and academia to model systems with detailed geometric features (e.g. stiffeners and curvature) while accommodating many nonlinear phenomena. FEA models may require thousands, or sometimes millions, of equations to describe the dynamics, so often times nonlinear reduced order modeling strategies are sought to speed up computational cost, which becomes especially useful for the computation of NNMs from these detailed FEA models. The numerical algorithm for NNMs requires time integration of the equations of motion (EOM), combined with shooting and pseudo-arclength continuation [3], and can be overly expensive for FEA models with many degrees-of-freedom (DOF). This paper proposes a methodology to approximate the NNMs of a full, geometrically nonlinear FEA model by first computing the nonlinear reduced order model (NLROM) equations, then computing the NNMs from these NLROM equations. The NNMs serve as a useful metric to gauge whether the NLROM equations converge with the various decisions used to build them.

The nonlinear normal mode was originally defined by Rosenberg [4] as a synchronous, periodic motion, or a vibration in unison, of the nonlinear equations of motion. More recently, Vakakis, Kerschen and others [5, 6] have extended this definition to include periodic motions where modal interactions may also occur by relaxing the synchronous restriction. According to their definition, which is the one used throughout this paper, a nonlinear normal mode is a *not necessarily synchronous periodic response of the undamped nonlinear equations of motion*. Each NNM by this definition describes how the resonant frequency and response of the structure changes as the

response amplitude (or energy) increases. Even though the properties of superposition and orthogonality do not apply to NNMs, they still provide a wealth of insight into the structure's behavior since they form the backbone of the systems nonlinear forced response [5, 6], and act as attractors for the lightly damped free response [7, 8]. Nonlinearities in a physical model can come in a variety of forms such as of large deformations, jointed connections, buckling, material constitutive laws, and contact. These nonlinear models introduce behavior such as frequency-energy dependence, localization, modal interactions and bifurcations. The nonlinear normal mode provides a new definition of a vibration mode that accounts for such salient nonlinear behavior, revealing many insights into the system.

Over the past few decades, many different methods have been developed to reduce linear elastic, geometrically nonlinear finite element models to a low order set of nonlinear modal equations using a truncated set of linear normal modes as the reduction basis. These reduced equations can be numerically integrated in the time domain at a significantly lower cost compared to direct integration of the full order equations while maintaining suitable accuracy. The works in [9, 10] compare a variety of these methods for geometrically nonlinear structures. There are two classifications of methods to determine the reduced, nonlinear modal equations: direct and indirect evaluation. Both of these methods produce equations of motion for the structure with a linear modal mass and stiffness and additional quadratic and cubic stiffness terms to account for the nonlinearity, which are coupled between the modal displacements. Direct evaluation methods manipulate the full order, nonlinear stiffness matrix in the finite element code [11-13] in order to generate the nonlinear stiffness terms. These approaches are not considered in this work since the nonlinear stiffness matrices within most commercial finite element packages are not in a functional form that is readily extracted. Indirect evaluation methods use a series of nonlinear static solutions to approximate the nonlinear coefficients. To the best of the authors' knowledge, Segalman et al. [14, 15] were the first to use such an approach by applying a series of static forces to a nonlinear FEA model to fit a Taylor series expansion of the nonlinear force-displacement relationship. This paper explores two different indirect evaluation methods for determining NLROMs of geometrically nonlinear FEA models.

The first indirect method, referred to as the *enforced displacement* (ED) procedure, was first developed by Muravyov and Rizzi [16]. The nonlinear FEA model is enforced to take the shape of a scaled linear mode shape or a combination of scaled linear mode shapes, and the reaction forces required to hold the shape are extracted. Using a set of displacement fields and reaction forces, the nonlinear stiffness coefficients in the nonlinear modal equations

are determined using the procedure outlined in [16]. For many thin-walled structures with geometric nonlinearity, the bending-membrane coupling must be accounted for explicitly with these reduced order models. When selecting the modal basis for the ED approach, it is important to include both bending and membrane modes in order to capture this coupling and accurately predict the response. Mignolet et al. [17] introduced the concept of a *dual mode* which captures the membrane motion caused by a bending mode. A similar *companion mode* method was developed by Holkamp et al. in [9, 18], but neither of these techniques were explored in this work.

The second approach is the applied loads procedure, which originated with McEwan [19] and is referred to as Implicit Condensation in [1]. A static force is applied to the nonlinear FEA model proportional to the shape, or a combination of shapes, of the linear modes in the basis set, and the resulting displacement fields are extracted. The set of statically applied forces and resulting displacements are used to fit the nonlinear stiffness coefficients in the reduced order model equations. Since forces are applied to the structure, the bending-membrane coupling is implicitly captured within the response and nonlinear stiffness terms, requiring that only the bending modes be included in the reduced basis set. If the axial displacements or the corresponding stresses and strains are of interest, then Hollkamp and Gordon's Implicit Condensation and Expansion (ICE) method can be used to recover the membrane motions [20]. Using this approach, an orthogonal set of membrane modes is identified that are quadratic functions of the bending coordinates and they are used to reconstruct the membrane motions that correspond to a given bending displacement. The membrane motions are found in a post processing step and hence their DOF are not included in the nonlinear modal equations of motion.

These indirect NLROM strategies have been found to be sensitive to several factors such as the amplitudes of the loads used to fit the nonlinear stiffness coefficients, or the type and number of modes included in the basis. The inaccuracies of the resulting fit may only be visible at certain response levels due to the amplitude dependence of the NLROM. Relatively few works discuss the difficulties that can be encountered when seeking an accurate NLROM, and this paper looks to explore these with the computed NNMs. The objective of this paper is twofold. The first is to approximate the NNMs of a full order model with geometric nonlinearity distributed throughout each of its elements using NLROMs to reduce the computational cost of the continuation algorithm in [3]. However, in order for these NNM approximations to be accurate, the NLROMs must accurately represent the full order system. Therefore, the second objective of this paper is to use the NNM as a metric to determine when the NLROM equations converge. Past works have validated NLROMs experimentally or numerically by comparing time responses or the power

spectrum of the response to a random input [1, 21-23]. In this paper, the NNMs computed from candidate NLROMs generated with either the ED or ICE method are compared to the NNMs of the full order FEA model, which are computed using the applied modal force (AMF) algorithm in [24]. The NNM offers a powerful metric to compare full and reduced order models since these solutions span a range of response amplitudes and are independent of any external forces. The effect of the load/displacement scaling factors and mode selection is explored and preprocessing procedures are recommended to assure that a valid NLROM is obtained in order to compute accurate NNMs of the full order model.

The rest of the paper is organized as follows. The theory behind the nonlinear reduced order modeling strategies is reviewed in Section II, and how the continuation algorithm is used to compute the NNMs. Section III discusses the scaling factors of the static loads and mode selection of the NLROMs when generating reduced order models. The two NLROM strategies are then demonstrated on two geometrically nonlinear finite element models in Section IV. A clamped-clamped beam model readily demonstrates some of the sensitivities of the NLROM methods. The NNMs of a finite element model of an exhaust panel cover are then presented in order to demonstrate the procedure on a realistic engineering structure. Section V presents the conclusions.

II. Theory

The discretized system of equations for an N degree-of-freedom (DOF) linear elastic, geometrically nonlinear finite element model can be written as

$$\mathbf{M}\ddot{\mathbf{x}} + \mathbf{K}\mathbf{x} + \mathbf{f}_{NL}(\mathbf{x}) = \mathbf{f}(t) \tag{1}$$

where $\mathbf{M}$ is the $N \times N$ mass matrix, $\mathbf{K}$ is the $N \times N$ linear stiffness matrix, $\mathbf{f}_{NL}(\mathbf{x})$ is the $N \times 1$ nonlinear restoring force vector, and $\mathbf{f}(t)$ is the $N \times 1$ external force vector. The $N \times 1$ vectors $\mathbf{x}$ and $\ddot{\mathbf{x}}$ are the displacement and acceleration, respectively. The NLROM procedures seek to reduce these undamped, nonlinear equations using the linear vibration modes as the reduction basis, which are found by solving the eigenvalue problem $(\mathbf{K} - \omega_r^2 \mathbf{M})\boldsymbol{\phi}_r$. A small set of mass normalized mode shapes approximate the kinematics of the EOM as,

$$\mathbf{x}(t) = \boldsymbol{\Phi}_m \mathbf{q}(t) \tag{2}$$

Each column in the $N \times m$ mode shape matrix, $\boldsymbol{\Phi}_m$, is a mass normalized mode shape vector, $\boldsymbol{\varphi}$, and $\mathbf{q}$ is an $m \times 1$ vector of time-dependent modal displacements. The reduced coordinate space $\mathbf{q}$ is significantly smaller that the physical coordinate space $\mathbf{x}$ (i.e. $m << N$).

In order to reduce the full order EOMs, Eq. (2) is substituted into Eq. (1) and premultiplied by $\boldsymbol{\Phi}_m^{\mathrm{T}}$ to assure that the residual error is orthogonal to the reduction basis (note that $(\,)^{\mathrm{T}}$ is the transpose operator). The reduced, nonlinear modal form of the r^{th} equation becomes

$$\ddot{q}_r + \omega_r^2 q_r + \theta_r\left(q_1, q_2, \ldots, q_m\right) = \boldsymbol{\varphi}_r^{\mathrm{T}} \mathbf{f}(t) \tag{3}$$

where ω_r is the linear natural frequency, and q_r is the r^{th} modal displacement. The nonlinear modal restoring force is given as

$$\theta_r(\mathbf{q}) = \boldsymbol{\varphi}_r^{\mathrm{T}} \mathbf{f}_{NL}\left(\boldsymbol{\Phi}_m \mathbf{q}\right) \tag{4}$$

The nonlinear restoring forces are a nonlinear function, $\theta_r(\mathbf{q})$, of the modal displacements. Prior works [9, 10] have shown that if the finite element model is linear elastic with geometric nonlinearities derived using quadratic strain-displacement relationships, the function $\theta_r(\mathbf{q})$ becomes a quadratic and cubic polynomial, given as

$$\theta_r(q_1, q_2, \ldots, q_m) = \sum_{i=1}^{m} \sum_{j=i}^{m} B_r(i,j) q_i q_j + \sum_{i=1}^{m} \sum_{j=i}^{m} \sum_{k=j}^{m} A_r(i,j,k) q_i q_j q_k \tag{5}$$

The coefficients B_r and A_r are the quadratic and cubic nonlinear stiffness terms, respectively, for the r^{th} nonlinear modal equation. If the full order EOM in Eq. (1) are known in closed form, then the nonlinear coefficients in Eq. (5) can be directly computed (referred as direct evaluation in [9]). However, in cases where the closed form equations are not explicitly available (e.g. within commercial finite element packages), an indirect approach must be used. The coefficients are approximated using either the ED or ICE methods using a series of nonlinear static solutions. Once these nonlinear stiffness terms are identified, the NLROM equations are given by Eqs. (3) and (5), providing a significant computational savings for response prediction compared to direct time integration.

For the two NLROM methods discussed in this work, the linear term was set to ω_r^2 and treated as a known value during the identification of B_r and A_r. Originally, McEwan used a regression analysis to solve for the nonlinear stiffness coefficients using a set of applied load cases [19]. Further development of the Implicit Condensation method led Gordon and Hollkamp [1] to develop a constrained method where the nonlinear stiffness coefficients are directly solved for with certain relations between some of the B_r and A_r terms in order to preserve symmetry in the nonlinear stiffness matrices. This constrained approach is used to determine the nonlinear coefficients for the ICE procedure, whereas the approach developed by Muravyov and Rizzi in [16] is used with the ED method.

A. Enforced Displacements Procedure

The enforced displacements procedure uses a set of prescribed displacements in the shape(s) of the linear modes in the basis in Eq. (2). In general, a multi-modal displacement can be written as

$$\mathbf{X}_c = \boldsymbol{\varphi}_1 \hat{q}_1 + \boldsymbol{\varphi}_2 \hat{q}_2 + \ldots + \boldsymbol{\varphi}_m \hat{q}_m \tag{6}$$

where $\mathbf{X}_c$ is an $N \times 1$ displacement vector, and $\hat{q}_r$ is the scaling factor for the r^{th} mode in the basis. In order to accurately estimate the ROM, the scaling factors should scale the deformation shape of each mode to a level that exercises the geometric nonlinearity in the structure. Using a commercial finite element software package, the resulting reaction forces, $\mathbf{F}_c$, are computed in response to the given displacement field. Then, the quasi-static representation of the NLROM for the r^{th} modal equation becomes

$$\omega_r^2 \hat{q}_r + \sum_{i=1}^{m} \sum_{j=i}^{m} B_r(i,j) \hat{q}_i \hat{q}_j + \sum_{i=1}^{m} \sum_{j=i}^{m} \sum_{k=j}^{m} A_r(i,j,k) \hat{q}_i \hat{q}_j \hat{q}_k = \boldsymbol{\varphi}_r^{\mathrm{T}} \mathbf{F}_c \tag{7}$$

The nonlinear stiffness coefficients are then solved for using the approach presented in [16] with a set of enforced displacement load cases that are in a combination of one, two or three modes in the basis set. The number of nonlinear static solutions, for $m > 3$, required by the ED method [10] is

$$2m + \frac{3m!}{2(m-2)!} + \frac{m!}{6(m-3)!} \tag{8}$$

B. Applied Loads Procedure or Implicit Condensation and Expansion

The applied loads procedure uses a set of static forces in the shape of the linear modes in order to find the nonlinear stiffness coefficients of the NLROM. For example, a multi-mode static force can be a combination of those forces that would excite any of the modes in the reduced basis, given as

$$\mathbf{F}_c = \mathbf{M}\left(\boldsymbol{\varphi}_1 \hat{f}_1 + \boldsymbol{\varphi}_2 \hat{f}_2 + \ldots + \boldsymbol{\varphi}_m \hat{f}_m\right) \tag{9}$$

where $\mathbf{F}_c$ is the vector of applied forces, and $\hat{f}_r$ is the force scaling factor for the r^{th} mode. Note that the previous works on the applied loads method did not mention the use of the mass matrix when computing the force vector, but it was used here and is needed to obtain a force that exactly isolates a single mode for a linear system. The force scaling factors can be varied to exercise the desired amount of geometric nonlinearity in the structure, as will be discussed further in Section III. The resulting static deformation, $\mathbf{x}_c$, can then be projected onto the linear modal coordinates as follows

$$q_r = \boldsymbol{\varphi}_r^{\mathrm{T}} \mathbf{M} \mathbf{x}_c \tag{10}$$

Using the quasi-static force displacement relationship in Eq. (7), one can then solve for the nonlinear stiffness coefficients with the constrained approach [1] using a set of these applied loads exercising the different modes in the basis. With the applied loads approach, the number of load permutations (for $m > 3$) required to generate the static response data [1] is given as

$$2m + 2\frac{m!}{(m-2)!} + \frac{4m!}{3(m-3)!} \tag{11}$$

C. Nonlinear Normal Modes of Nonlinear Reduced Order Models

Once the NLROM equations are identified using either the ED or ICE methods, the NNMs of the NLROM can be computed and these can then be assumed to approximate the NNMs of the full order finite element model. For the NLROMs given by Eqs. (3) and (5), there exist at least m nonlinear normal modes that are each extensions of the linear modes in the basis (at low energy or response amplitudes). The pseudo-arclength continuation algorithm in [3] initiates the nonlinear normal mode at a linear mode solution, and the predictor-corrector type algorithm traces the

periodic solutions as the amplitude of the response increases. The method relies on the shooting technique to find the periodic solutions of the NLROM, using the shooting function

$$\mathbf{H}\left(T,\mathbf{q}_0,\dot{\mathbf{q}}_0\right)=\begin{Bmatrix}\mathbf{q}\left(T,\mathbf{q}_0,\dot{\mathbf{q}}_0\right)\\ \dot{\mathbf{q}}\left(T,\mathbf{q}_0,\dot{\mathbf{q}}_0\right)\end{Bmatrix}-\begin{Bmatrix}\mathbf{q}_0\\ \dot{\mathbf{q}}_0\end{Bmatrix}=\mathbf{0} \tag{12}$$

A periodic motion described by the integration period T, initial modal displacement $\mathbf{q}_0$, and initial modal velocity $\dot{\mathbf{q}}_0$ that satisfies the shooting function to a given numerical tolerance is deemed a valid NNM. The algorithm in [3] iterates on these variables (T, $\mathbf{q}_0$, $\dot{\mathbf{q}}_0$) using the Newton-Raphson method to search for a response that satisfies Eq. (12). Once a periodic solution is found, the solution is stored and the algorithm predicts a new solution along a line tangent to the current branch. The correction step is repeated by adjusting the predicted solution until the shooting function is again satisfied.

One advantage to this approach is that it can handle strong nonlinearities since each periodic solution is exact to a given integration tolerance. Unfortunately, the cost of the algorithm grows in proportion to the number of DOF in the model. The shooting and continuation techniques require the Jacobian of the nonlinear equations at each prediction and correction step, which is not readily exported from commercial finite element software. One could use finite differences to compute the gradients, but those become prohibitively expensive for high order systems (such as the detailed finite element models of interest). The AMF method in [24] reduces the number of continuation variables used to compute the nonlinear modes of a full order finite element model using the same pseudo-arclength continuation algorithm in [3], yet it is still quite expensive for many practical applications. NLROMs have the advantage of being far less expensive to integrate compared to the full finite element model, making the NNM computation very efficient. Furthermore, the Jacobian of the NLROM can be derived analytically from Eqs. (3) and (5), so the method in [3] could be used to further speed up computations. Hence, this could be a very efficient means of computing the NNMs of geometrically nonlinear structures. The only question is whether the NLROM is an accurate representation of the structure of interest.

III. Computing Accurate NLROMs

When generating an NLROM, mode selection and static load scaling factors can greatly affect the accuracy. These decisions are exploited when comparing the NNMs computed from these modal equations, revealing whether

or not the NLROM is representative of the full order model. Previous works [1, 16] have provided basic guidelines for these decisions when creating the NLROM, and a discussion of these is presented below.

A. Mode Selection

It is important to include all of the important modes in the reduced basis set when building the reduced order model, otherwise the NLROM will not be adequate for its intended purpose. For a linear system, one must include all of the excitable modes in a frequency range of interest to accurately capture the response of the model. The addition of nonlinearity into the full order model requires further considerations. For example, geometric nonlinearity essentially couples the underlying linear modes of the structure, so additional modes outside the typical bandwidth of interest may be needed to account for such interactions. A low frequency mode can potentially excite a higher frequency mode outside of the desired excitation bandwidth and if the coupling is strong, these high frequency modes should be included in the basis set. For example, if the structure's nonlinearity is cubic, then it is well known that a periodic input at a frequency ω may excite modes at higher harmonics such as 3ω, 5ω and hence one may need to consider modes outside the bandwidth of the input forces to accurately capture the response of the structure.

The method used to build the NLROM (either ED or ICE) also influences which modes to include. For example, the coupling between the bending and membrane motions causes "stretching" that is not always accurately captured with a set of low frequency bending modes. When using the enforced displacements procedure the high frequency membrane modes must be explicitly included in the basis set to account for this coupling. On the other hand, with the Implicit Condensation and Expansion method, membrane modes do not need to be included since the softening due to membrane stretching is implicitly captured during the identification of the nonlinear stiffness coefficients. Nonlinear systems are also known to exhibit internal resonances, where a nonlinear mode at a given energy level can exchange energy with a different nonlinear mode [6]. In order to capture this phenomenon, the NLROM must include the linear modes that are involved in the modal interaction. In theory, an infinite number of internal resonances may exist for even the simplest systems, but certain modal interactions will likely be more important than others.

A few methods have been proposed to identify a modal basis for the NLROM. For example, Rizzi and his colleagues presented an approach in [22, 23] that uses a short dynamic response to a representative loading to determine a modal basis. In this paper, the authors offer an alternate approach to identify which linear modes are

nonlinearly coupled to each of the bending modes of interest based on a nonlinear static solution of the finite element model. A force proportional to a single, linear mode shape is scaled with a constant factor, $\hat{f}_r$, chosen to ensure the nonlinearity is excited, and applied to the FEA model. A nonlinear static solution then reveals which membrane and bending modes couple to that given mode, independent of any external forces the structure may experience. Specifically, the FEA model computes the solution to the following equation, where excitation is applied to the r^{th} linear mode,

$$\mathbf{K}\mathbf{x} + \mathbf{f}_{NL}(\mathbf{x}) = \mathbf{M}\boldsymbol{\varphi}_r \hat{f}_r \tag{13}$$

By computing the displacement that results from the static force, the modal amplitudes of the candidate modes due to the force are computed as

$$\mathbf{q} = \boldsymbol{\Phi}^{\mathrm{T}}\mathbf{M}\mathbf{x} \tag{14}$$

If the force is small (in the linear regime), the applied force will result in a displacement exactly in the r^{th} mode shape and hence only q_r will be nonzero. For larger forces the nonlinear static solution reveals the natural coupling between that mode and other bending and membrane modes due to geometric nonlinearity. The modal amplitudes in Eq. (14) guide the selection of the appropriate modes to supplement each linear mode that falls in the frequency range of interest. Consider the computation of the r^{th} nonlinear normal mode initiated at the r^{th} linear mode at low energy. The NNM can be checked for convergence by adding the linear mode with the next largest value in the $\mathbf{q}$ vector to the NLROM and then recomputing the NNM. If the additional mode improves the resulting NNM, then the mode should be included in the basis set. This procedure helps identify when a sufficient basis set has been selected to capture the r^{th} NNM. This can be used for both the enforced displacements and Implicit Condensation procedures, and will be demonstrated in Section IV.

B. Scaling Factors for Multi-Mode Models

The scaling factors in Eqs. (6) and (9) govern the degree to which the nonlinearity in the structure is activated in the response data used to fit the nonlinear stiffness coefficients. If the scale factors are too small, the nonlinearity in the response may be on the order of computational noise leading to numerical difficulty when attempting to

determine the polynomial coefficients A_r and B_r. Similar problems may result if one mode is excited far more or far less than the others. This section discusses the suggested approaches for setting the scale factors for the ED and ICE methods.

1. Enforced Displacement Scaling Factors

Here, the authors propose a new method, termed constant modal displacement (CD) factor, which sets the scaling factors $\hat{q}_r$ in Eq. (6) for each mode in a meaningful way. The modal scale factor required to displace the r^{th} mode to a certain maximum displacement (in physical coordinates), $w_{\max,r}$, can be written as

$$\hat{q}_r = CD_r = \frac{w_{\max,r}}{\boldsymbol{\varphi}_{r,\max}} \tag{15}$$

where $\boldsymbol{\varphi}_{r,\max}$ is the maximum displacement value of the r^{th} mass normalized mode shape. Note that generally the maximum displacement occurs at a different displacement DOF for each mode. Also, different values of $w_{\max,r}$ may be chosen depending on the mode of interest. For example, if the scaling factor is for a bending mode, choosing a $w_{\max,r}$ value on the order of the thickness of the structure will typically assure that the displacements exercise the nonlinearity. For an axial mode, then a value on the order of a fraction of the thickness (a tenth or hundredth) could be used since these modes do not behave nonlinearly and unreasonably large forces would be needed to cause them to displace by one thickness, perhaps introducing numerical ill-conditioning into the ROM fitting process.

The works in [16, 25] explain that the ED NLROM obtained is insensitive to the amplitude of $\hat{q}_r$, and hence the scale factors chosen. For the enforced displacement procedure, they proposed using the same scaling factor for all modes included in Eq. (6). This method will be referred to as the constant modal scale (CS) factor method, where the scale factors are chosen to be the same for all modes and are determined based on the maximum displacement of the lowest order bending mode as

$$\hat{q}_r = CS_r = CD_1 \tag{16}$$

where CD_1 is given by Eq. (15). It is suggested that $w_{\max,1}$ is chosen to be physically reasonable for the lowest frequency bending mode and within the range of displacements expected in the application of interest. The results in Section IV will explore the results obtained by each approach and discuss some of the issues that arise.

2. Applied Load Scaling Factors

For the applied loads procedure, Gordon and Hollkamp specify scaling factors based on the amount of force required to achieve a certain maximum displacement for the linear system [1]. The equation for the scaling factor of the r^{th} mode shape based on the loading in Eq. (9) is formulated as

$$\hat{f}_r = CLD_r = \frac{w_{\max,r}}{\boldsymbol{\varphi}_{r,\max}} \omega_r^2 \tag{17}$$

This method of scaling is termed constant linear displacement (CLD). Note that this equation is slightly different than the equation presented in [1] due to the mass matrix being pre-multiplied by the force vector in Eq. (9). The desired linear displacement for each mode should sufficiently excite the geometric nonlinearity. Typically a displacement on the order of one thickness is used for the primary, low frequency modes [1], however, higher frequency modes tend to require a lower $w_{\max,r}$ value. It is important to select a displacement amplitude, $w_{\max,r}$, large enough to overcome the linear range of the response, but small enough to avoid convergence issues with the finite element solution. One recommendation for determining $w_{\max,r}$ for each mode is to compute the nonlinear static solution to the force in Eq. (13), and find the resulting maximum displacement, $w_{\max,r,NL}$. The ratio of the nonlinear to linear maximum displacement is defined as

$$\gamma_r = \frac{w_{\max,r,NL}}{w_{\max,r}} \tag{18}$$

Typically, the ratio for γ_r should be between 0.8 and 0.95 for hardening nonlinearities to ensure that sufficient nonlinearity is excited [1].

Another important issue arises when determining the load cases that involve multiple modes simultaneously. After determining the CLD scaling factors for each mode, a reduction of these amplitudes is recommended here

when applying a static force in a combination of two or three modes. For example, when applying a load in the combination of modes 1 and 2, the CLD factors should be reduced by a factor of two such that the loading becomes

$$\mathbf{F}_c = \mathbf{M}\left(\boldsymbol{\varphi}_1 \cdot \frac{1}{2} \hat{f}_1 + \boldsymbol{\varphi}_2 \cdot \frac{1}{2} \hat{f}_2 \right) \tag{19}$$

Similarly for combinations of three modes, each CLD factor should be reduced by a factor of three. This ensures that the applied forces do not exceed desired displacement levels, and contaminate the fit of the nonlinear stiffness coefficients. This method is termed the reduction factor (RF) method when presenting the results in Section IV.

C. Multiple Displacement/Load Case Sets

Thus far, the discussion for both NLROM procedures has been limited to using a single set of load cases with some scaling method. One displacement/load case set can be used [1, 16] in order to fit the nonlinear stiffness coefficients, however McEwan mentions the use of different load case sets in order to exercise the nonlinearity to a greater or lesser extent [19]. Muravyov and Rizzi found that the nonlinear stiffness coefficients did not change significantly as the maximum displacement was varied [16] and conclude that the coefficients are insensitive to the displacement amplitudes [25, 26]. Gordon and Hollkamp discuss multiple load case sets and mention that using different scaling factors for the different load case sets can provide more robust models, especially when considering curved structures [1]. The multiple displacement/load case sets will not be explored in this paper, but the authors' experiences to date suggest that the largest load case dominates the NLROM.

IV. Results

The ED and ICE nonlinear reduced order modeling strategies were evaluated using two different geometrically nonlinear finite element models. The NLROMs were first created for each model with different modes and scaling factors, and then the NNMs were computed and compared to gain insight into the convergence, and also provide an approximate NNM of the full model. The first system was a flat planar beam with clamped-clamped boundary conditions. The results from the beam were compared with the NNMs computed directly from the full order finite element software, with no reduction, using the applied modal force (AMF) method in [24]. In practice, it is hoped that it will not be necessary to have this (computationally expensive) truth data, but that one will be able to choose a ROM based on how the NNMs converge as the NLROMs are refined. However, for the purposes of this paper it is

informative to have these reference NNMs that satisfy the FEA model precisely. The effects of scaling factors and mode selection for the ED and ICE methods are highlighted with this study. Using the lessons learned from the clamped-clamped beam, the method was applied to a more complicated FEA model of an exhaust cover plate with 15,708 DOF.

A. Clamped-Clamped Beam

The geometrically nonlinear beam exhibited stiffening/hardening nonlinearities caused by the coupling between bending and membrane motions for large transverse displacements. The beam model was identical to that studied in [9], and had the following dimensions: 228.6 mm (9 in.) long, with a cross section of 12.7 mm (0.5 in.) wide by 0.787 mm (0.031 in.) thick. It was modeled with forty B31 beam elements in Abaqus®, resulting in 117 DOF. It was constructed of steel with a Young's modulus of 204.8 GPa (29,700 ksi), a shear modulus of 80.0 GPa (11,600 ksi), and a mass density of 7,870 kg/m^3 ($7.36\cdot10^{-4}$ lb-s^2/in^4).

First, the modal coupling due to the geometric nonlinearity was investigated by applying a static force proportional to the first five symmetric bending modes, and projecting the displacement onto the mass normalized linear modes using Eq. (14). As in [9], we presume that the anti-symmetric modes will not be excited and hence are not of interest. The force was scaled for each of the modes using the CLD method in Eq. (17) with a $w_{\max,r}$ value of 0.787 mm (0.031 in.), or 1 beam thickness. The magnitude of the resulting modal amplitudes were normalized to the largest amplitude, and sorted in descending order in Table 1. A static force applied to excite the first linear mode revealed nonlinear coupling to other symmetric bending modes (modes 3, 5, 7, 9, etc..). In addition, anti-symmetric axial modes 26, 39, 45 and 47 were also found to be coupled to the first bending mode. The results suggested which axial/membrane modes to augment with the bending modes for the ED procedure, as well as which bending modes to successively include in the basis set, for either the ED or ICE method, in order to get convergence of the NLROM.

Table 1. Relative modal amplitude due to a static force applied to excite the linear mode shapes of the clamped-clamped beam.

Force in Mode 1		**Force in Mode 3**		**Force in Mode 5**		**Force in Mode 7**		**Force in Mode 9**	
Mode #	Amp	Mode #	Amp	Mode #	Amp	Mode #	Amp	Mode #	Amp
1	1	3	1	5	1	7	1	9	1
3	$9.3\cdot10^{-3}$	1	$5.7\cdot10^{-1}$	1	$6.8\cdot10^{-1}$	1	$7.2\cdot10^{-1}$	1	$7.4\cdot10^{-1}$
5	$1.3\cdot10^{-3}$	5	$2.4\cdot10^{-2}$	3	$2.0\cdot10^{-1}$	3	$2.6\cdot10^{-1}$	3	$2.9\cdot10^{-1}$
39	$5.0\cdot10^{-4}$	7	$7.2\cdot10^{-3}$	7	$2.6\cdot10^{-2}$	5	$1.1\cdot10^{-1}$	5	$1.4\cdot10^{-1}$
7	$3.1\cdot10^{-4}$	9	$2.7\cdot10^{-3}$	9	$1.1\cdot10^{-2}$	9	$2.5\cdot10^{-2}$	7	$7.6\cdot10^{-2}$

26	$2.4\cdot10^{-4}$	47	$1.5\cdot10^{-3}$	11	$5.3\cdot10^{-3}$	11	$1.3\cdot10^{-2}$	11	$2.3\cdot10^{-2}$
9	$9.9\cdot10^{-5}$	11	$1.1\cdot10^{-3}$	13	$2.7\cdot10^{-3}$	13	$7.1\cdot10^{-3}$	13	$1.4\cdot10^{-2}$
45	$6.7\cdot10^{-5}$	45	$9.8\cdot10^{-4}$	51	$2.6\cdot10^{-3}$	15	$4.1\cdot10^{-3}$	15	$8.2\cdot10^{-3}$
11	$3.9\cdot10^{-5}$	13	$5.5\cdot10^{-4}$	49	$1.9\cdot10^{-3}$	55	$3.6\cdot10^{-3}$	17	$5.1\cdot10^{-3}$
13	$1.8\cdot10^{-5}$	49	$4.1\cdot10^{-4}$	15	$1.5\cdot10^{-3}$	53	$2.9\cdot10^{-3}$	59	$4.7\cdot10^{-3}$
47	$1.7\cdot10^{-5}$	15	$2.9\cdot10^{-4}$	26	$1.1\cdot10^{-3}$	17	$2.5\cdot10^{-3}$	57	$3.9\cdot10^{-3}$

1. One-Mode NLROMs

A one-mode NLROM was first generated using the ED and ICE procedures, and the NNMs were computed from the resulting equations and are shown in Fig. 1. The CLD factor was used with the ICE method, where the $w_{\max,1}$ value was set to a displacement of 0.5 times the beam thickness, or 0.394 mm (0.016 in.), such that the ratio of nonlinear to linear displacement at the midpoint was γ_1=0.88. A CD scale factor that produced a displacement where $w_{\max,1}$ was 3 times the thickness was used for the ED NLROM. The reason for selecting these optimal values is addressed later in this subsection. The legend for each NLROM in Fig. 1 uses the following convention: "NLROM strategy (modes included) scaling method ($w_{\max,r}$/beam thickness x Number of modes with that ratio)." For example, the last line in the legend in Fig. 1 represents an enforced displacement NLROM (ED) which includes modes 1, 26, and 39 using the constant displacement scale factor method (CD) with $w_{\max,1}$ set to 3 times the beam thickness for the first mode in the basis set (mode 1) and $w_{\max,26}$ and $w_{\max,39}$ set to 0.01 times the beam thickness for the two (x2) axial modes (modes 26 and 39).

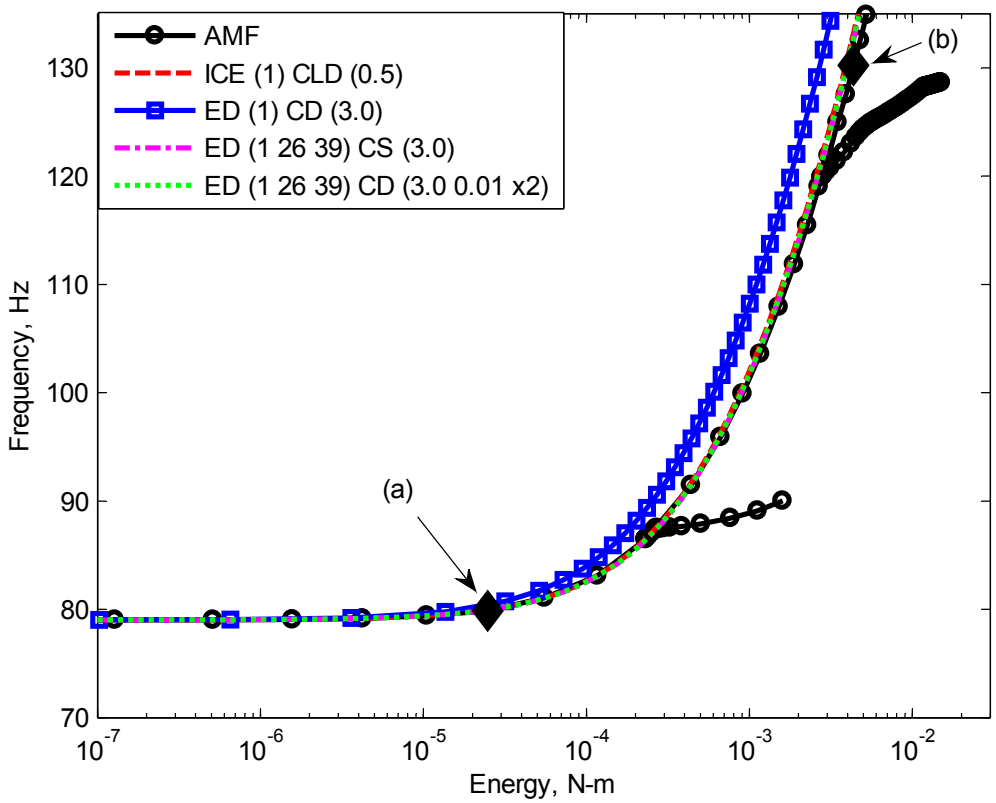

Figure 1. Frequency-energy plot of NNM 1 of the clamped-clamped beam model with various NLROM strategies. Deformations of solutions (a) and (b) are plotted in Fig. 2.

The NNM is shown on the frequency-energy plane, where each point along the curve represents a periodic solution to the nonlinear equations. The fundamental frequency on the vertical axis was computed from the minimum period of the response (higher harmonics were generally observed as energy increased). The energy along the horizontal axis was computed as the total energy, kinetic plus potential, of the system during the periodic response. The results in Fig. 1 show that a one-mode NLROM created using the ICE procedure (dashed red) accurately captured the backbone of the first NNM when compared to the truth results from AMF (black circles). At higher energies (above 0.003 N-m), the one-mode ICE NLROM was slightly stiffer than the true NNM. As expected, a comparable one-mode model created using the enforced displacement procedure (blue squares) was much stiffer and hence much less accurate than the ICE NLROM over the whole energy range due to the lack of membrane-softening in the basis of the ED NLROM. It is well known that membrane modes must be included in an ED NLROM in order to obtain accurate results; the results above quantify the error that is incurred when the membrane modes are neglected.

The ED NLROM was improved by adding the first two anti-symmetric axial modes to the basis set (modes 26 and 39), as determined by the coupling in Table 1. Two different scaling methods were used when adding these modes: CS scaling, and also CD scaling with $w_{\max,r}$ set to 3 times and 0.01 times the beam thickness for the first bending mode and the associated axial modes, respectively. After adding these two axial modes, either of the ED NLROMs were as accurate as the one-mode ICE NLROM. This illustrates the fact that the membrane displacements must be included in the basis set for the ED method in order to accurately capture the nonlinear stiffness, whereas the ICE method implicitly captured these effects. For this NNM no difference was seen between the results obtained using the CD (short dashed green) and CS (dashed dot magenta) scaling methods. Hence, when using the enforced displacements approach the higher frequency axial modes can be displaced much less than the bending modes during the static load cases and produce an accurate NLROM.

All of these approaches gave an excellent estimate for the backbone of NNM 1, even though the NLROMs only included the first bending mode. The ED procedure was at a slight disadvantage since it required the axial modes explicitly in the basis set, but in this case these modes were easily identified using a statically applied force in the shape of the first bending mode as shown in Table 1. The dual modes method proposed by Mignolet et al. [17] would likely include similar axial effects, but this approach was not explored in this paper. Each NLROM procedure captured the bending-membrane coupling caused by geometric nonlinearity, and was examined more thoroughly by looking at the deformations at different points along the NNM branch. The plot in Fig. 2 shows the maximum deformation shape (e.g. when the velocity of the periodic response was zero) at the points marked (a) and (b) in Fig. 1 for the ICE and ED methods, as well as the AMF truth results. The position of each node is plotted in mm, and the color bar shows the log of the ratio of in-plane displacement to transverse displacement at each node.

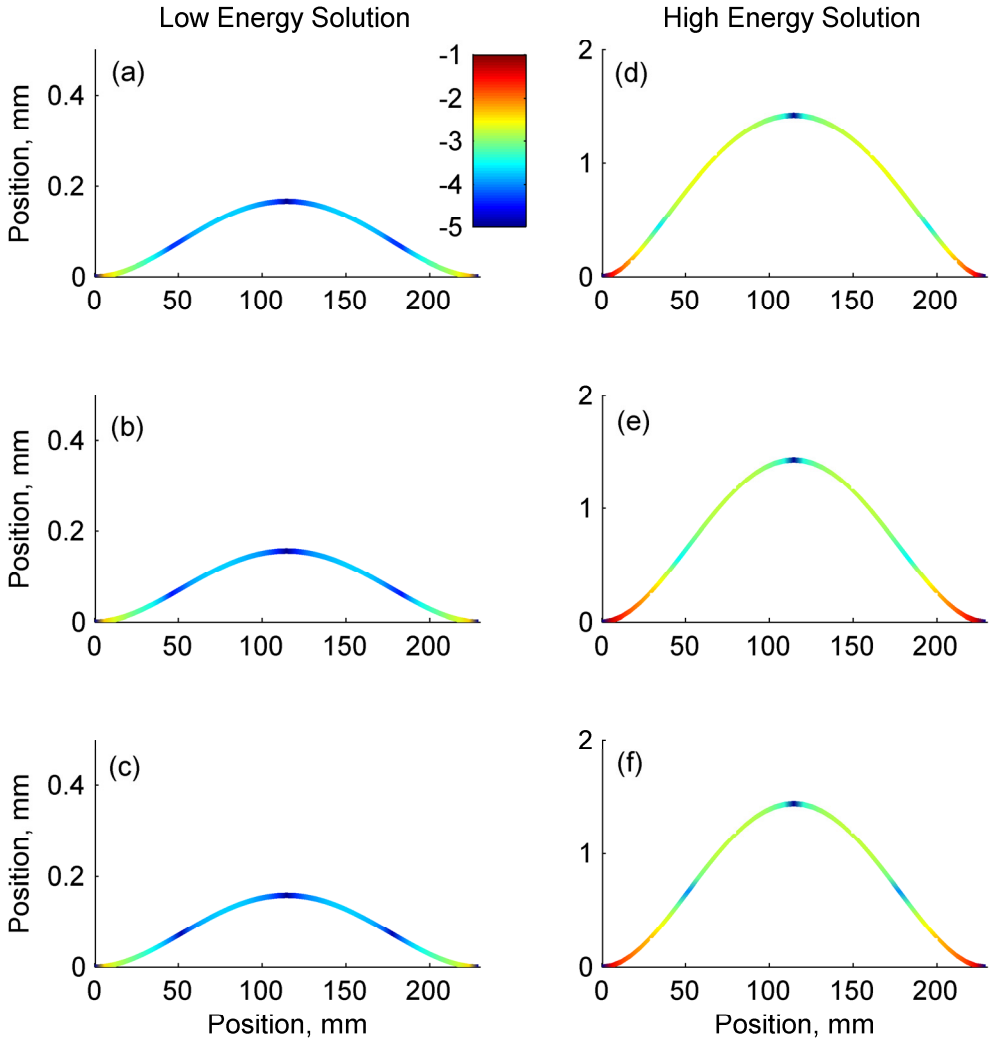

Figure 2. Deformation shapes of NNM 1 in Fig. 1 at low (left column) and high (right column) energy computed using the (a, d) AMF method, (b, e) ICE (1) CLD (0.5), and (c, f) ED (1 26 39) CD (3.0 0.01 x2). The color bar gives the log of the ratio of in-plane displacement to transverse displacement at each node.

At low energy (left column), the deformation shapes predicted by the NLROMs and full FEA model were dominated by the first linear bending mode shape of the beam, with little membrane stretching near the clamped ends. This agrees with the fact that the NNM converged to the linearized mode of the system at low energy, since the amplitude of the bending motion was not large enough to induce much bending-membrane coupling. The solution at high energy (right column), near 130 Hz on the FEP, showed significant contribution of nonlinearity in the periodic response. Each of the deformations in Fig. 2 (right column) show that the bending-membrane coupling was much more significant than the lower energy solution. The NLROMs predicted the nonlinear deformation

reasonably well at high energy, but looking closely one can see that they both differ slightly from the AMF response; the AMF solution appears to "flatten" near the midpoint, suggesting that the third bending mode was beginning to contribute to the NNM. Also, the color bar shows that the axial deformation predicted by ED and ICE does not exactly agree with that obtained by AMF; the node points in the axial displacement occur about 2 cm closer to the clamped ends in the AMF result. These discrepancies perhaps explain the differences between the FEPs at higher energy in Fig. 1. The lack of higher order bending modes also explains why neither of these models captured the "tongues" that emanated from the FEPs in the AMF solution. These deviations are known as internal resonances, or modal interactions, and occur when two or more nonlinear normal modes interact with one another.

A few NLROMs were generated with larger and smaller scaling factors in order to demonstrate the inaccuracy of the reduced equations when the proper scaling amplitude was not chosen for the static load cases. The FEPs of the first NNM in Fig. 3 show results from ICE ROMs with CLD where the $w_{\max,1}$ value was set to a displacement of 0.001 and 30.0 times the beam thickness, and ED ROMs with CD scaling factors where the first bending mode displaced with $w_{\max,1}$ of 0.5 and 100.0 times the thickness. These scale factors were chosen to illustrate how sensitive/insensitive the methods can be in various cases. Due to the hardening nature of the NNM, the $A_1(1,1,1)$ stiffness term dictates the "bend" of the NNM curve, so the different scaling amplitudes affect the fit of this value. For the ICE procedure, the FEP miscalculates the backbone of NNM 1 drastically when the force amplitude was not large enough to excite the nonlinearity (dashed red), and was only just beginning to diverge when the force was too large (short dashed green). Using the ED approach, applying a displacement that is only marginally less than the beam thickness (blue squares) clearly misses the behavior of the full order model, and even predicts softening behavior around 0.006 N-m! On the other hand, even when the first mode is displaced far more than is optimal, the ED NLROM (dashed dot magenta) produces a backbone that diverges a little from the AMF solution. The NNMs are clearly sensitive to the scaling, and hence one can use an analysis like this for each bending mode in the basis set to determine the range of scaling factors that seem to give the most consistent or reasonable results. In the next subsection, additional modes are added and similar studies were done to select the optimal scaling values for the appropriate bending and axial modes used in either ROM procedure. Those results show that the multi-mode ROMs are even more sensitive to the scaling.

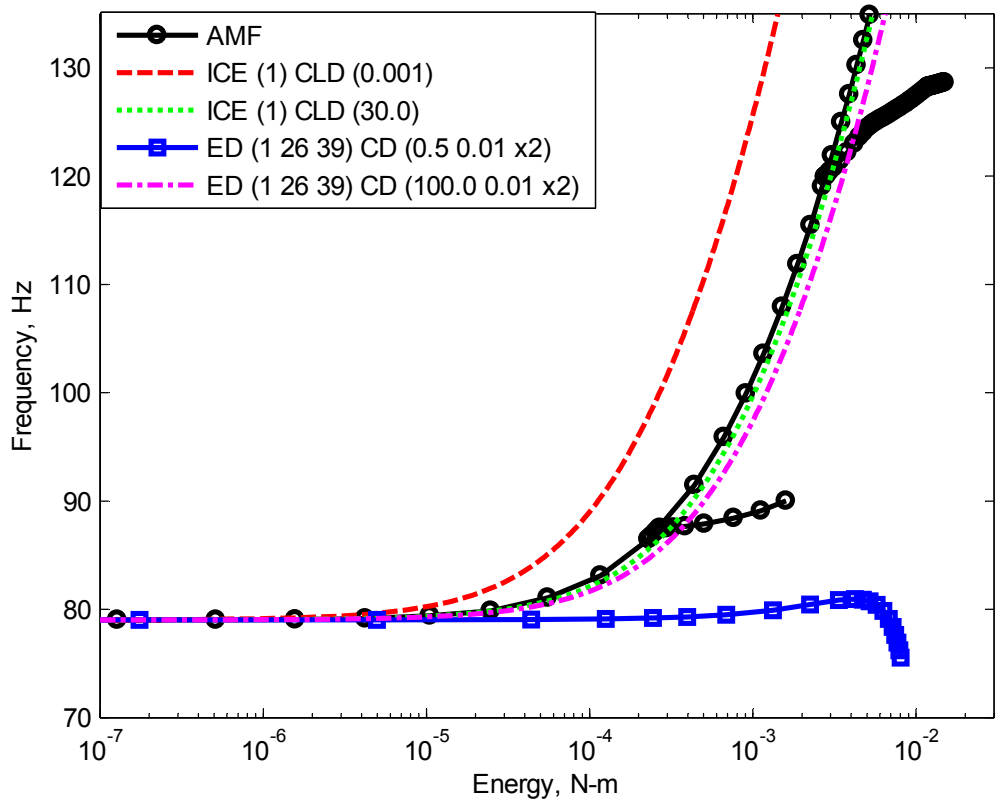

Figure 3. Frequency-energy plot of NNM 1 of the clamped-clamped beam model with various NLROM strategies.

2. Multi-Mode NLROMs

More bending modes were included in the basis set to improve the accuracy of the NLROMs and to allow them to capture the internal resonances. The tongue at 88 Hz in the FEP in Fig. 1 (AMF, dotted black) was a 1:5 internal resonance, representing an interaction between the 1st and 3rd NNMs. For each solution along the tongue, the 3rd mode oscillated at 5 times the frequency of the 1st mode. The natural frequency of the third linear bending mode is 427.5 Hz, which is not commensurate with the linear natural frequency of the first bending mode (79 Hz), but as the frequency of NNM 1 increased, the integer ratio between the two frequencies became commensurate with a 5 to 1 ratio, resulting in a modal interaction. The second internal resonance, near 120 Hz, started as a 1:4 interaction with the third bending mode. As energy increased, the fifth bending mode began to oscillate at a 1:9 ratio, simultaneously as the third mode vibrated at a 1:4 ratio. At even higher energy, the seventh mode began to contribute at a 1:16 ratio, along with the previous interactions. These types of internal resonances, between modes whose linear frequencies are not commensurate, has received relatively little attention in the literature [6].

In order to capture this behavior with the NLROMs, all of the modes involved in the interaction must be included in the basis set. The ED procedure was used with additional bending and axial modes. Based on the results in Table 1, bending modes 3, 5, and 7 were added due to the nonlinear coupling to the first bending mode. For each higher frequency bending mode, two of the dominant anti-symmetric axial modes coupled to that bending mode were also added to the basis. The first NNM, computed from multi-mode ED NLROMs using various mode combinations and scaling methods is shown in Fig. 4. The axial modes were again displaced at a much lower fraction of the beam thickness (0.01 times the thickness) with the CD scaling method.

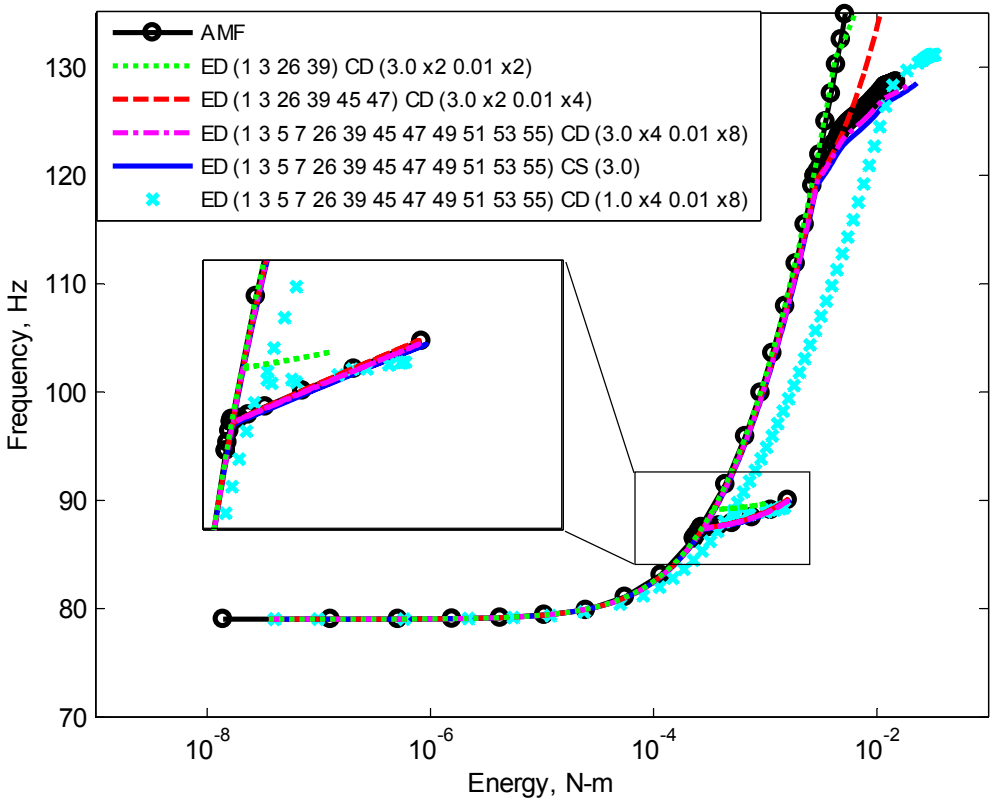

Figure 4. Frequency-energy plot of NNM 1 of the clamped-clamped beam model with ED NLROM strategy with higher frequency bending and axial modes.

The various results presented here illustrate several issues that were discovered and which must be addressed to obtain an accurate estimate of the NNM. First consider the ED (1 3 26 39) ROM shown in dashed green. At very high energies this ROM estimated the NNM backbone more accurately than the ED (1 26 39) ROM in Fig. 1, confirming the importance of the third bending mode at these energies. However, this NLROM still does not capture the internal resonance near 88 Hz where linear modes 1 and 3 interact. By simply adding the two anti-symmetric axial modes that were most strongly coupled to the third bending mode (modes 45 and 47), the NLROM

(dashed red) accurately computed its interaction with the third NNM near 88 Hz. The additional axial modes, which coupled to the third bending mode, helped soften the third NNM (not shown here), which influenced the modal interaction on the first NNM branch. Note that trial and error revealed that two axial modes were needed for each bending mode for this problem. NLROMs were also created including only one anti-symmetric axial mode per bending mode and they did not compare as well with the AMF solution.

As expected, neither of the ROMs considered thus far (the ED (1 3 26 39) and ED (1 3 26 39 45 47) NLROMs) accurately captured the second internal resonance near 120 Hz, since it involved bending modes 5 and 7, which were not included in the basis. By adding these modes (5 and 7) with the appropriate axial modes (49, 51, 53, 55) and using the CD scaling method, we obtained a result (dashed dot magenta) that had nearly converged to the AMF truth NNM and now captured the second internal resonance near 120 Hz. This illustrates the importance of including an adequate number of bending modes in the basis set, and augmenting these with the appropriate axial modes.

Two other cases are also presented to illustrate the effect of scaling. A 12-mode ED NLROM was created with the CS scaling, ED () CS (3.0) (solid blue) and found to agree very well with the result when CD scaling was used, ED () CD (3.0×4 0.01×8) (dashed dot magenta). Either method seems to produce an accurate NLROM. Even though the CS method worked well, one objection to this approach was that it automatically assigned the scaling amplitude to the other modes in the basis. These automatically assigned values could potentially cause higher order modes to be displaced too little, causing the nonlinearity to not be excited and the nonlinear stiffness coefficients to be poorly fit. The cyan x's in Fig. 4 shows an example of this using an identical 12-mode basis with the CD method, but where the bending modes were displaced 1 times the beam thickness rather than three times. This NLROM did not accurately represent the backbone of NNM 1, nor the internal resonances. It appears that the bending modes were not displaced enough in this case to adequately excite the nonlinearity, and as a result the NLROM coefficients cannot be accurately estimated. This shows that the scaling for the static displacements must be carefully selected in order to generate an accurate NLROM. Other cases were explored, and the results seemed to show that the scaling values were insensitive to the displacement level as long as the displacement adequately excited the geometric nonlinearity.

Next, the convergence of the ICE method was evaluated as bending modes were added to the basis set, while using the CLD scaling method for the static loads to fit the nonlinear stiffness coefficients. The FEPs of NNM 1 in Fig. 5 were computed from NLROMs with modes 1, 3, modes 1, 3, 5, 7 and modes 1, 3, 5, 7, 9, 11. (Recall that the

axial modes do not need to be included in the basis set when using the ICE method.) Each bending mode used a CLD factor of 0.5 times the thickness, except for mode 11 which used a value of 0.1 time the thickness. These values were selected in order to keep the nonlinear to linear displacement ratio γ_r near 0.9.

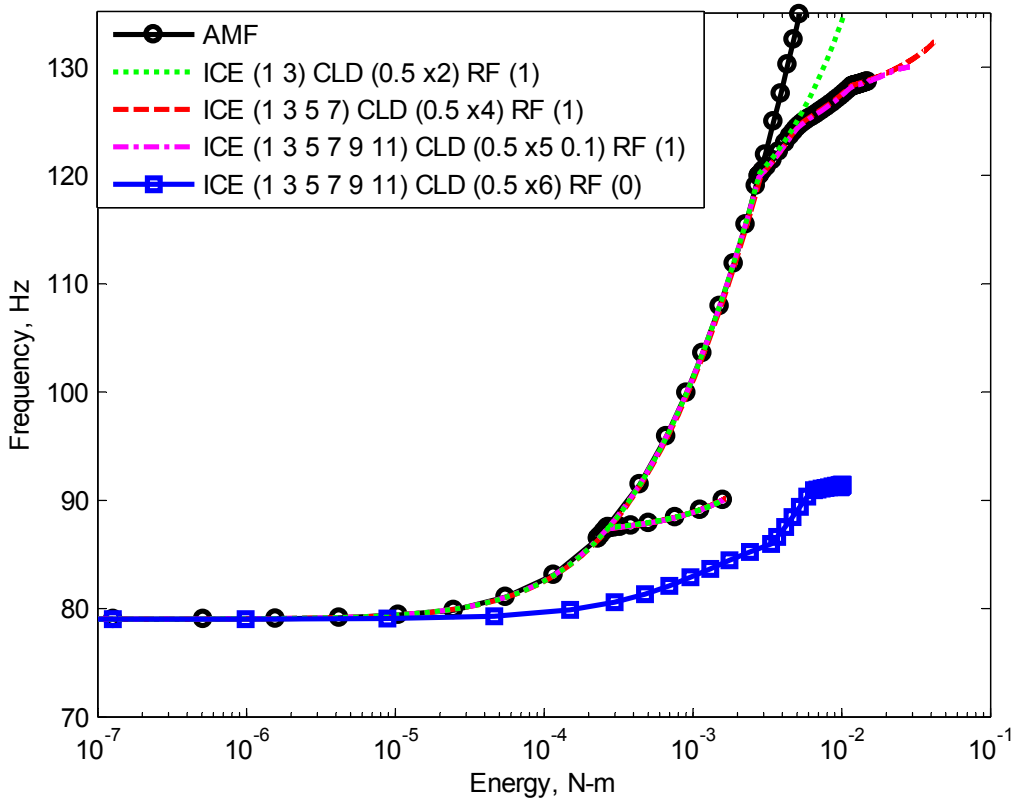

Figure 5. Frequency-energy plot of NNM 1 of the clamped-clamped beam model with ICE NLROM strategy using higher frequency bending modes.

The NNMs for the ICE method with CLD scaling in Fig. 5 revealed that the first NNM converged quickly along the main backbone, as the two-mode NLROM (short dashed green) captured the first internal resonance near 88 Hz as soon as the third bending mode was added. The first NNM converged on the second internal resonance near 120 Hz as well as other modes were added to the NLROM. Recall that at higher energies along this tongue, modes 5 and 7 began to interact with the first NNM. In order to capture this behavior, each of the higher frequency modes needed to be included in the basis. Overall, when the NLROM used CLD scaling factors and the RF method was used to keep the loads small when forces were applied in the shape of several modes simultaneously (e.g. RF (1) in the legend means that this feature was used), the NLROMs converged to the AMF solution of NNM 1 of the beam. Note that the bending modes used to build these equations did not contain any axial deformation (as is the case for flat

structures), so in order to recover these membrane effects in physical coordinates, the expansion method described in [20] must be used.

The NLROM with the RF method (dashed dot magenta) and the appropriate scaling (e.g. mode 11 with CLD (0.1)) produced an NNM that agreed very well with the AMF results, even along the second internal resonance. The ICE method showed considerable sensitivity to the scaling amplitudes when not using the reduction factor, RF (0), as illustrated by the last line in Fig. 5, where the 6-mode basis (modes 1, 3, 5, 7, 9, 11) was used with a CLD factor of 0.5 times the thickness for mode 11 and no reduction factor (blue squares). In the authors' experience to date, the RF was more robust and produced more consistent results as the NNMs seemed to be less sensitive to amplitude of the scale factors.

Finally, the next two higher frequency NNMs were computed with the ICE and ED NLROMs and compared to the results with the AMF algorithm, as shown in Fig. 6. Each NLROM was capable of computing the NNM, which is an extension of the linear mode at low energy, as long as that mode was included in the basis set. NNMs 3 and 5 computed with the two NLROM procedures in Fig. 6 agree very well with the AMF solution along the backbone, in fact they practically overlay each other in the FEP. A small discrepancy exists between the ED NLROM (dashed red) and AMF (black circles) at the internal resonance near 680 Hz in NNM 3. This was a 5:1 modal interaction with the NNM 9, and since the ED NLROM does not include the ninth bending mode in the basis set, it was unable to capture this internal resonance, but otherwise the two ROMs gave almost indistinguishable results for these NNMs. The procedure that was used to determine which modes were needed in the NLROMs to characterize the first NNM could, in principle, be used to capture any other NNMs that are of interest.

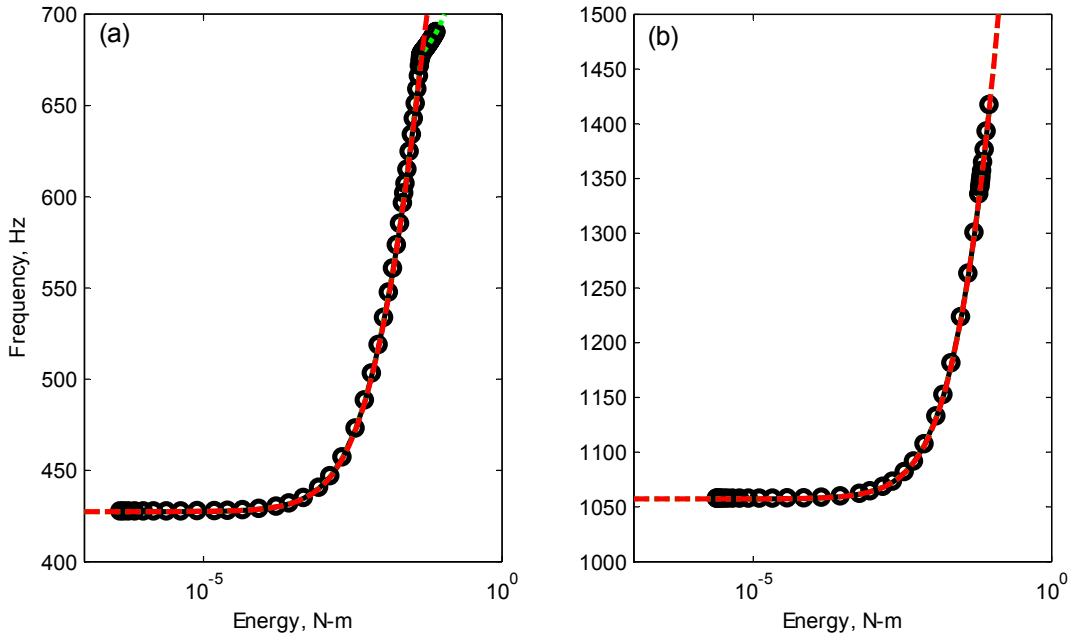

Figure 6. Frequency-energy plot of (a) NNM 3 and (b) NNM 5 of the clamped-clamped beam model with (black circles) the AMF algorithm, (short dashed green) ICE (1 3 5 7 9 11) CLD (0.5 x5 0.1) RF (1) and (dashed red) ED (1 3 5 7 26 39 45 47 49 51 53 55) CD (3.0 x4 0.01 x8).

B. Exhaust Cover Plate

The NLROMs were also used to compute the first NNM of a larger, more realistic FEA model of an exhaust cover plate that exhibited geometric nonlinearity during laboratory tests. The model reduction strategy becomes even more appealing for this system since it has many more degrees of freedom than the beam studied earlier. The mesh for this model is shown in Fig. 7. The plate was 317.5 mm (12.5 inches) in diameter, and was constructed of structural steel with a mass density of 7,800 kg/m^3 ($7.29 \cdot 10^{-4}$ lb-s^2/in^4) and a Young's modulus of 208 GPa (30,160 ksi). The plate was modeled in Abaqus® with 899 S8R shell elements, with a uniform thickness of 1.5 mm (0.059 inches), resulting in a total of 15,708 DOF. Each DOF along the bottom ring of the plate was fixed in all translations and rotations, modeling the relatively rigid boundary to which the plate is welded.

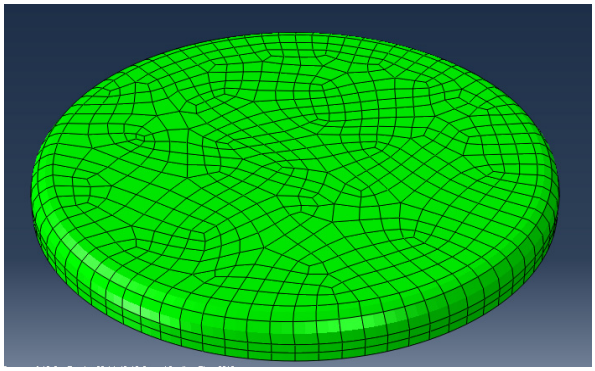

Figure 7. Finite element model of a geometrically nonlinear exhaust cover plate.

A static force was applied to the FEA model that would have displaced the first linear mode a maximum of 1.5 mm (0.059 inches), or 1 times the plate thickness. The displacement revealed static coupling to higher frequency modes, and is shown in Table 2 in descending order of relative modal amplitude. The first five of these linear mode shapes are plotted in Fig. 8. These identified mode shapes serve as candidate modes to include in the NLROM basis. Note that no purely axial or membrane modes appeared to be coupled to the first bending mode, although mode 156 is predominantly axial. Similar studies of curved beams and curved panels have shown that axial modes often cease to be distinct from the bending modes when there is curvature in the structure [27-29].

Table 2. Relative modal amplitude due to a static force applied to excite the first linear mode of the exhaust plate, and the corresponding linear natural frequency.

Mode #	1	6	156	15	30	175	51	74
Amp	1.00	$6.8\cdot10^{-3}$	$4.0\cdot10^{-3}$	$2.4\cdot10^{-3}$	$1.5\cdot10^{-3}$	$1.5\cdot10^{-3}$	$9.5\cdot10^{-4}$	$5.6\cdot10^{-4}$
Frequency, Hz	156.4	607.5	10,770	1,358	2,402	11,650	3,731	5,328

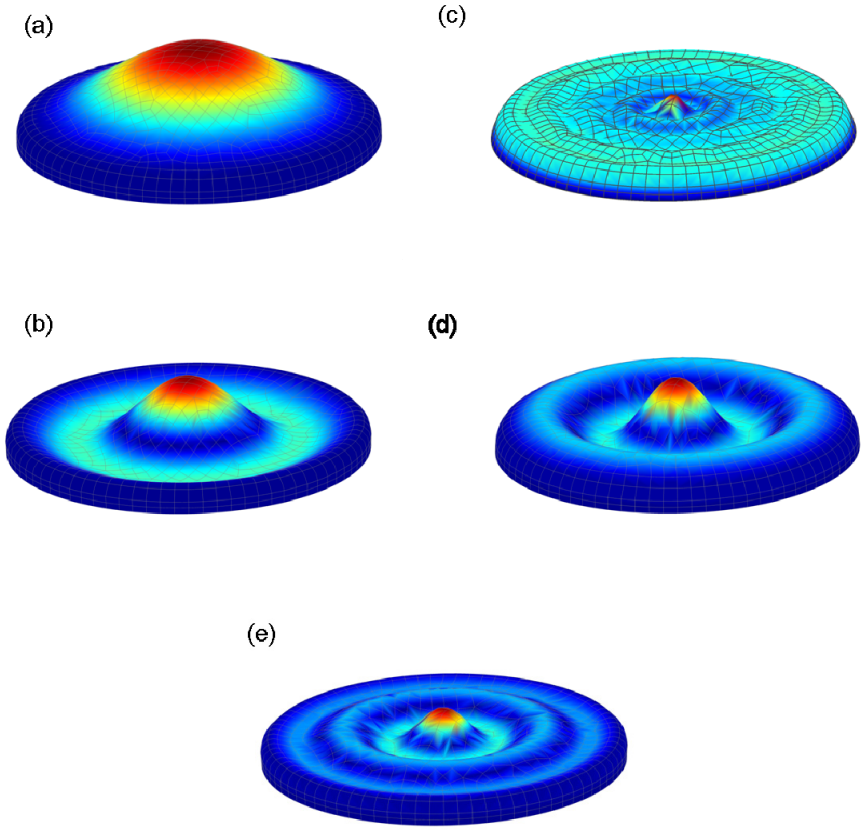

Figure 8. Linear mode shapes of exhaust cover plate model for (a) mode 1, (b) mode 6, (c) mode 156, (d) mode 15, and (e) mode 30.

The ICE and ED strategies were used to build NLROMs in order compute the first NNM of the exhaust plate. The AMF algorithm was also used to determine the first NNM of this system, albeit at significant computational expense, in order to provide a truth result against which to compare each NLROM. Based on the best practices observed for the beam system studied in the previous subsection, the CD scaling approach where $w_{\max,r}$ of 3 times the thickness was used with the ED method to produce the NNMs shown in Fig. 9. The CLD scaling with the RF was used with the ICE method and these results are shown in Fig. 10. For the CLD scaling factors with the ICE method, it was determined that using a scaling value $w_{\max,1}$ equal to 1.5 mm (0.059 inches), or 1 times the plate thickness, was reasonable for the first bending mode, since the plate's curved edges make this structure's boundary more compliant than the clamped beam's. Higher frequency modes used a lower fraction of the thickness in order to keep the nonlinear to linear displacement ratio γ_r near 0.9.

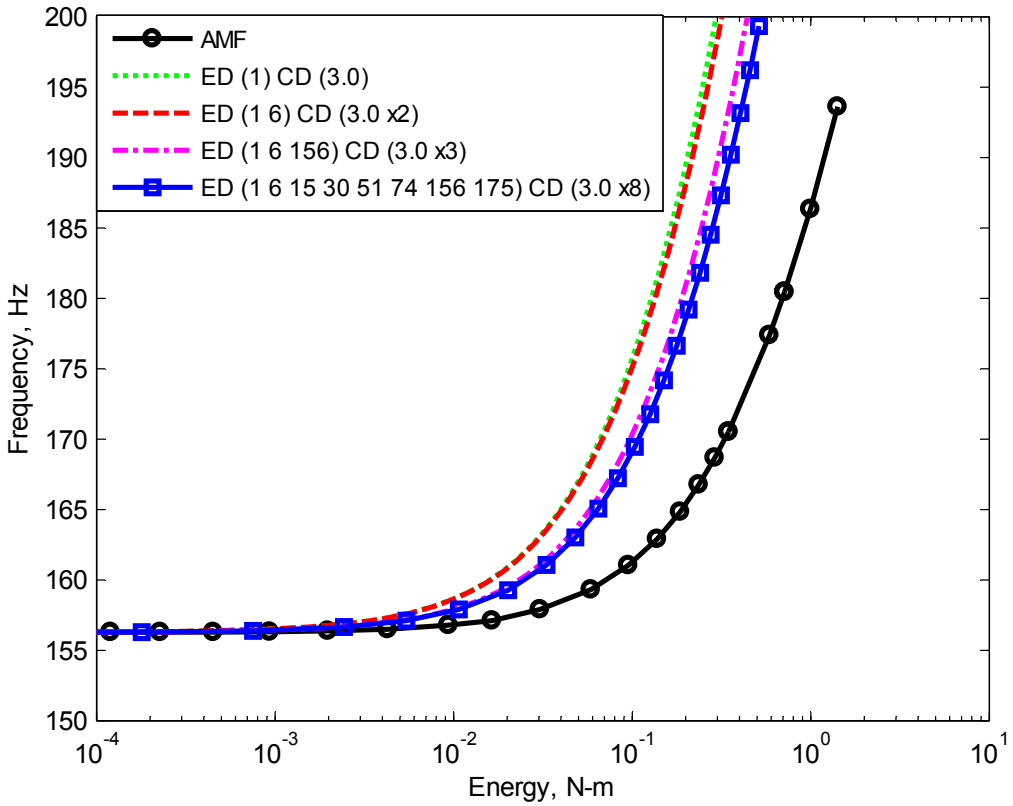

Figure 9. Frequency-energy plot of NNM 1 of the exhaust cover plate model with ED NLROM strategy using higher frequency bending modes.

The ED method did not perform as well for this system as it did for the beam. A single-mode NLROM was greatly in error, yet results for the first NNM improved somewhat as additional modes were added to the ED basis. Even after including the eight modes that were most strongly coupled to the first bending mode, as shown in Table 2, the FEP was off by nearly an order of magnitude in energy at 190 Hz. The FEA model of the clamped-clamped beam showed that including axial, or membrane, type modes greatly improved the accuracy of the ED NLROM. However, no pure membrane modes existed for the exhaust cover plate due to its slight curvature, so this remedy was not available.

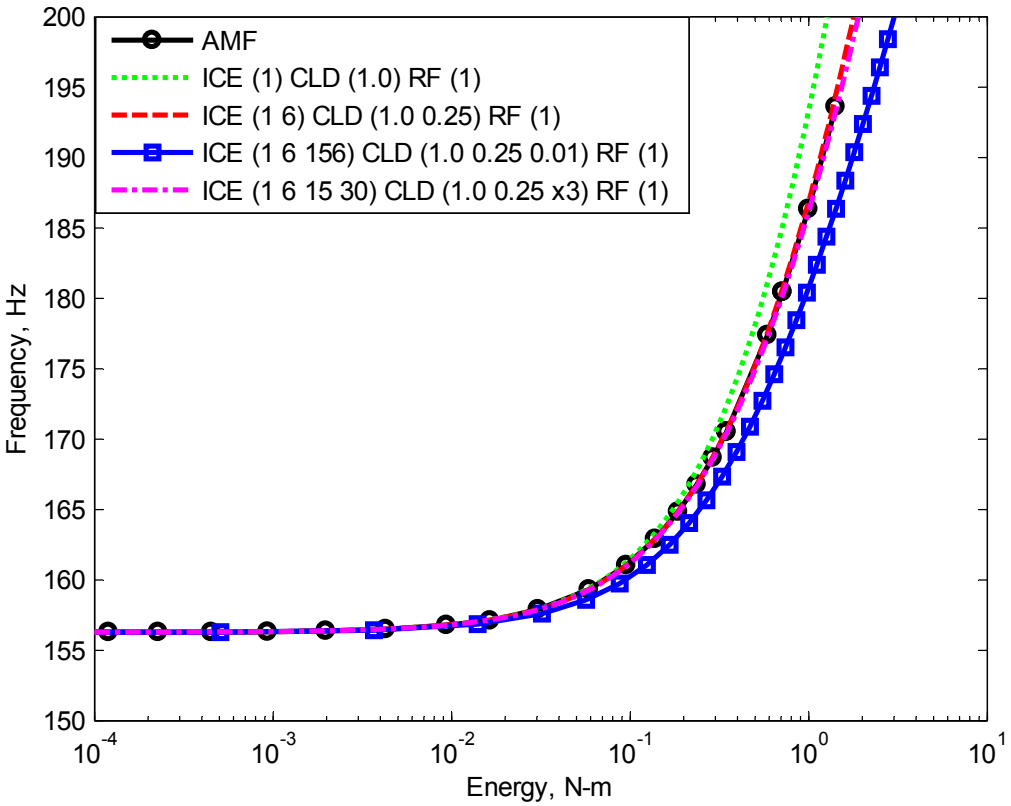

Figure 10. Frequency-energy plot of NNM 1 of the exhaust cover plate model with ICE NLROM strategy using higher frequency bending modes.

The NNM estimated by a one-mode NLROM (short dashed green) constructed using the ICE method was only slightly in error, and it quickly converged to the AMF result when mode 6 was added to the basis (dashed red). The sixth bending mode had a strong coupling to the first NNM, and hence it is not surprising that this mode had an important effect. Using this NLROM, the first NNM could be computed much more efficiently than by AMF; only about 15 minutes were needed to solve the nonlinear static load cases, generate the NLROM, and compute the first NNM branch. In contrast, running the AMF algorithm on the full model took approximately 4 days. The ICE approach offers an excellent alternative to AMF for finite element models such as these.

Two other cases are also shown to illustrate a potential pitfall. When the next dominant mode, mode 156, was added to the ICE basis set (blue squares), the first NNM diverged. When including this mode in the basis, the FEA model would not converge on the static solution unless the amplitude was low, although a CLD with $w_{\max,156}$ equal to 0.01 times the plate thickness resulted in a nonlinear to linear displacement ratio γ_{156} of 0.98. It was decided that mode 156 should be removed from the basis set, and the next two modes (15 and 30) included instead, producing the

result shown with the dashed dot magenta line. The resulting four-mode NLROM again predicted the first NNM very accurately. This example highlights the importance of mode selection with the CLD scaling method. The fact that mode 156 has a much higher frequency leads one to believe that this mode only needs to be included implicitly (as done with ICE method), and should not be included explicitly in the basis set. Based on these results, the ICE method seemed to be better suited for systems with many DOF, as long as the modes are scaled appropriately and the correct modes were added to the basis.

VI. Conclusions

In this work, two nonlinear reduced order modeling strategies were used to represent geometrically nonlinear finite element models with a low order set of nonlinear modal equations. These indirect methods use the static response of the nonlinear structure to fit a nonlinear function that involves quadratic and cubic polynomial combinations of the modal displacements. The first approach, termed Implicit Condensation and Expansion, applies a static force to excite the linear modes shapes within the nonlinear FEA model and uses the resulting displacements to fit the modal model. The second approach is the enforced displacement method, where instead the nonlinear structure is displaced into the shape of a combination of linear modes, and the reaction forces are then used to fit the modal model. This work showed that the NNMs can be used as a metric to determine whether the NLROM equations correctly capture the physics over a range of frequency and energy. This helps guide the decisions used to generate the NLROMs, such as which modes to include in the basis set, as well as the scaling methods to use when generating the static load cases. The NNMs were invaluable in this regard. The NLROMs themselves are comprised of a collection of stiffness coefficients with widely varying units for linear, quadratic and cubic terms. The sheer number of terms can also be daunting; for a 12 mode NLROM there are 5,304 terms, and an error in any one term could invalidate the entire transient response. NNMs are relatively inexpensive to compute from the NLROM and they readily show the differences and similarities between the two NLROMs and give tremendous physical insight into how the responses of the NLROMs might differ.

Regardless of the NLROM strategy, these results show that the analyst must consider the scaling factors and mode selection in order to get an accurate representation of the full finite element model. For the systems studied in this work, the constant displacement (CD) scaling method gave slightly better results for the enforced displacement procedure, while the constant linear displacement (CLD) method with the reduction factor (RF) worked best for

Implicit Condensation and Expansion. It is also worth noting that these procedures are a slight shift from the existing literature. Both methods require the user to define the level of force/displacement for each mode in the basis set, and these levels seem to depend on the model and mode of interest. For this reason, computing the NNMs of the resulting NLROM equations offers insight into the effect of these decisions, helping the analyst decide when convergence has been achieved.

One disadvantage of the ED method is the requirement to include appropriate axial modes for each bending mode in the basis set, causing the ED method to have more DOF than ICE. This increases the size of the NLROM and the expense required to compute its response, although it is still dramatically less expensive than the original finite element model. On the other hand, there are practical advantages to the ED method since all of the important axial motions are captured within the NLROM formulation, whereas the axial motions have to be recovered in a post processing step with the ICE method. Fortunately, the results have shown that a simple static force in the shape of a particular linear vibration mode can reveal which modes should be added to the ED NLROM basis. The ICE NLROMs converged quickly for each finite element model studied, requiring only a few modes. The ED method converged with the beam with relatively few modes, but did not converge for the exhaust cover plate. The enforced displacement method with dual modes may have provided a basis with better modal convergence, but this was not explored in this paper and will be in future work.

To the best of the authors' knowledge, this is the first work to use nonlinear normal modes to evaluate the convergence of a nonlinear reduced order model. The authors believe that this comparison has great promise for other model reduction strategies. Previous works focused on comparing the transient response of the structure or the power spectra of the response when a random input is applied, but those each depend on a forcing function and the initial conditions. In contrast, the NNMs are unique solutions to the undamped equations of motion over a range of energy (or range of forcing levels), and they are relatively easy to compute using recently developed continuation algorithms. This work has shown that the NNMs serve as a valuable metric to assess the convergence of a NLROM equations.

Acknowledgments

This work was supported by the Air Force Office of Scientific Research, Award # FA9550-11-1-0035, under the Multi-Scale Structural Mechanics and Prognosis program managed by David Stargel. The authors would also like to

thank Peter Penegor and David Nickel from Cummins Emissions Solutions for providing the geometry of the exhaust cover plate. The authors are also grateful to Stephen Rizzi for the help he provided in implementing the ED method and in choosing scale factors for that method.

References

[1] R. W. Gordon and J. J. Hollkamp, "Reduced-Order Models for Acoustic Response Prediction," Air Force Research Laboratory (AFRL), Wright-Patterson Air Force Base, OH AFRL-RB-WP-TR-2011-3040, 2011.

[2] G. Tzong and S. L. Liguore, "Verification Studies on Hypersonic Structure Thermal/Acoustic Response and Life Prediction Methods," presented at the 54th AIAA/ASME/ASCE/AHS/ASC Structures, Structural Dynamics, and Materials Conference, 2013.

[3] M. Peeters, R. Viguié, G. Sérandour, G. Kerschen, and J. C. Golinval, "Nonlinear normal modes, Part II: Toward a practical computation using numerical continuation techniques," *Mechanical Systems and Signal Processing,* vol. 23, pp. 195-216, 2009.

[4] R. M. Rosenberg, "Normal modes of nonlinear dual-mode systems," *Journal of Applied Mechanics,* vol. 27, pp. 263–268, 1960.

[5] A. F. Vakakis, "Non-linear normal modes (NNMs) and their applications in vibration theory: an overview," *Mechanical Systems and Signal Processing,* vol. 11, pp. 3-22, 1997.

[6] G. Kerschen, M. Peeters, J. C. Golinval, and A. F. Vakakis, "Nonlinear normal modes. Part I. A useful framework for the structural dynamicist," *Mechanical Systems and Signal Processing,* vol. 23, pp. 170-94, 2009.

[7] H. A. Ardeh and M. S. Allen, "Investigating Cases of Jump Phenomena in a Nonlinear Oscillatory System," presented at the 31st International Modal Analysis Conference (IMAC XXXI), Garden Grove, California, 2013.

[8] M. Peeters, G. Kerschen, and J. C. Golinval, "Dynamic testing of nonlinear vibrating structures using nonlinear normal modes," *Journal of Sound and Vibration,* vol. 330, pp. 486-509, 2011.

[9] J. J. Hollkamp, R. W. Gordon, and S. M. Spottswood, "Nonlinear modal models for sonic fatigue response prediction: a comparison of methods," *Journal of Sound and Vibration,* vol. 284, pp. 1145-63, 2005.

[10] M. P. Mignolet, A. Przekop, S. A. Rizzi, and S. M. Spottswood, "A review of indirect/non-intrusive reduced order modeling of nonlinear geometric structures," *Journal of Sound and Vibration,* vol. 332, pp. 2437-2460, 2013.

[11] M. Nash, "Nonlinear Structural Dynamics by Finite Element Modal Synthesis," in *Department of Aeronautics* vol. Ph.D. Dissertation, ed: Imperial College, The University of London, 1977.

[12] Y. Shi and C. Mei, "A finite element time domain modal formulation for large amplitude free vibrations of beams and plates," *Journal of Sound and Vibration,* vol. 193, pp. 453-464, 1996.

[13] P. Tiso, E. Jansen, and M. Abdalla, "Reduction method for finite element nonlinear dynamic analysis of shells," *AIAA Journal,* vol. 49, pp. 2295-2304, 2011.

[14] D. J. Segalman and C. R. Dohrmann, "A Method for Calculating the Dynamics of Rotating Flexible Structures, Part 1: Derivation," *Journal of Vibration and Acoustics,* vol. 118, pp. 313-317, 1996.

[15] D. J. Segalman, C. R. Dohrmann, and A. M. Slavin, "A Method for Calculating the Dynamics of Rotating Flexible Structures, Part 2: Example Calculations," *Journal of Vibration and Acoustics,* vol. 118, pp. 318-322, 1996.

[16] A. A. Muravyov and S. A. Rizzi, "Determination of nonlinear stiffness with application to random vibration of geometrically nonlinear structures," *Computers & Structures,* vol. 81, pp. 1513-1523, 2003.

[17] M. P. Mignolet, A. G. Radu, and X. Gao, "Validation of reduced order modeling for the prediction of the response and fatigue life of panels subjected to thermo-acoustic effects," in *Proceedings of the 8th International Conference on Recent Advances in Structural Dynamics*, 2003, pp. 14-16.

[18] J. J. Hollkamp, R. W. Gordon, and S. M. Spottswood, "Nonlinear sonic fatigue response prediction from finite element modal models: a comparison with experiments," in *Proceedings of the 44th AIAA/ASME/ASCE/AHS/ASC Structures, Structural Dynamics, and Materials Conference*, 2003.

[19] M. I. McEwan, J. R. Wright, J. E. Cooper, and A. Y. T. Leung, "A Combined Modal/Finite Element Analysis Technique for the Dynamic Response of a Non-linear Beam to Harmonic Excitation," *Journal of Sound and Vibration,* vol. 243, pp. 601-624, 2001.

[20] J. J. Hollkamp and R. W. Gordon, "Reduced-order models for nonlinear response prediction: Implicit condensation and expansion," *Journal of Sound and Vibration,* vol. 318, pp. 1139-1153, 2008.

[21] R. W. Gordon, J. J. Hollkamp, and S. M. Spottswood, "Nonlinear response of a clamped-clamped beam to random base excitation," presented at the Eighth International Conference on Recent Advances in Structural Dynamics, University of Southampton, Southampton, UK, 2003.

[22] A. Przekop, X. Guo, and S. A. Rizzi, "Alternative modal basis selection procedures for reduced-order nonlinear random response simulation," *Journal of Sound and Vibration,* vol. 331, pp. 4005-4024, 2012.

[23] S. A. Rizzi and A. Przekop, "System identification-guided basis selection for reduced-order nonlinear response analysis," *Journal of Sound and Vibration,* vol. 315, pp. 467-485, 2008.

[24] R. J. Kuether and M. S. Allen, "A numerical approach to directly compute nonlinear normal modes of geometrically nonlinear finite element models," *Mechanical Systems and Signal Processing,* vol. 46, pp. 1-15, 2014.

[25] S. A. Rizzi and A. Przekop, "The Effect of Basis Selection on Static and Random Acoustic Response Prediction Using a Nonlinear Modal Simulation," NASA TP-2005-213943, 2005.

[26] S. A. Rizzi and A. Przekop, "Estimation of Sonic Fatigue by Reduced-Order Finite Element Based Analyses," presented at the IX International Conference on Recent Advances in Structural Dynamics, Southampton, UK, 2006.

[27] R. W. Gordon and J. J. Hollkamp, "Reduced-Order Modeling of the Random Response of Curved Beams using Implicit Condensation," in *47th AIAA/ASME/ASCE/AHS/ASC*

Structures, Structural Dynamics, and Materials Conference, Newport, Rhode Island, 2006.

[28] S. M. Spottswood, R. W. Gordon, and J. J. Hollkamp, "On the use of Reduced-Order Models for a Shallow Curved Beam under Combined Loading," in *49th AIAA/ASME/ASCE/AHS/ASC Structures, Structural Dynamics, and Materials Conference*, Schaumburg, Illinois, 2008.

[29] R. W. Gordon and J. J. Hollkamp, "Reduced-Order Models for Acoustic Response Prediction of a Curved Panel," in *52nd AIAA/ASME/ASCE/AHS/ASC Structures, Structural Dynamics, and Materials Conference*, Denver, Colorado, 2011.